Optimization of Shrimp Shell Waste Deproteinization and Deacetylation for Chitosan Production Using a Fractional Factorial Design (FFD)

Atiqa Kherbache[1*], Fatma Youcefi[1], Linda Ouided Ouahab[1], Dehas Ouided[2], Achref Cherifi[2]

[1]Laboratory of Functional Agro-Systems and Technologies of Agronomic Sectors, Abou Bakr Belkaid University, BP.119.Tlemcen 13000, Algeria.

[2]Laboratory of Anti-Corrosion, Materials-Environment, and Structure (LAMES), University of 20 August, 1955 Skikda 21000, Algeria.

[2]Research Center In Industrial Technology: Additive manufacturing Research Unit, Industrial Zone A15. Setif 19000, Algeria.

Corresponding author Email: fatmayoucefi65@gmail.com

Receive 12/10/2023 ; Accepted 05/01/2024; Published 19/01/2024

Abstract

Chitosan is deacetylated chitin, the second most common polysaccharide after cellulose. The diverse applications of chitosan are directly linked to the properties of the polymer, which vary depending on the extraction process. This study aimed to investigate the factors that influence the deproteinization and deacetylation of chitin and to elucidate their effect on the residual protein level, the level of deacetylation (DD), and the yield of extracted material. The selected responses were studied using a 25-1 fractional factorial design with five factors and two levels of variation. The factors tested were A NaOH concentration, B = reaction time, C temperature, D = Particle size, and E = Solid/Liquid ratio. Using the ANOVA regression equation gives a coefficient of determination R2 = (99.62%, 99.72%, and 99.90%) for the residual protein level, the deacetylation (DD), and yield, respectively, indicating the precision of the predicted model. The minimum of residual proteins, the maximum deacetylation DD% and yield% reached under those conditions corresponds to the concentration of NaOH (20%,40%), temperature (40°C,129.88°C), reaction time (15.03,60min), particle size of (0.3,01mm) and Solid/Liquid ratio of (1/10.02,1/15 g/ml). After carrying out the validation test, the chitosan obtained presents a yield, ash rate, residual proteins, a DD%, solubility, crystallinity, and a molecular weight of 16.16±0.22, 0.124±0.002, 2.08±0.05%, 87.13±0.16%, 97.02±0.09%, 44.32%, and 107.47±0.44KDa respectively.

Keywords: Chitin; Chitosan; Deproteinization; Deacetylation; Experimental design; Optimum conditions.

Tob Regul Sci.™ 2024;10(1): 1878 - 1901

DOI: doi.org/10.18001/TRS.10.1.118

Introduction

The need for seafood has led to a significant expansion of the seafood processing industry in recent years. The food-processing sector, like to other sectors in its field, generates substantial amounts of waste. Approximately 6 to 8 million tons of shellfish trash (including crab, shrimp, and lobster) are generated globally each year (FAO, 2019).

Managing the substantial quantity of waste generated by shrimp processing companies is a significant issue, particularly in poor nations, where most waste is disposed of in garbage and oceans. This is an important environmental issue as it directly affects the populations of endangered animals. For wealthy nations, removing waste might incur high costs, rendering it economically impractical for many companies. Therefore, it is imperative to devise creative measures to reduce environmental damage and optimize financial gains (Kannan, Gariepy and Raghavan, 2017).

The composition of shrimp waste is minerals "$CaCO_3$" (30–50%), (30–40%) of protein, and (20–30%) of chitin and its major derivative, chitosan, have multiple applications (Nouri and al ., 2016). Some applications necessitate specific structures, and the effectiveness has been demonstrated to depend on the purity and consistency of chitin quality. Many organic and inorganic substances are strongly associated with chitin in shrimp shells. These substances must be removed to get the highly pure chitin needed for biological applications (Nidheesh and Suresh, 2015).

The conventional process to produce chitosan from chitin includes three steps: first, demineralization in acid solutions; second, deproteinization in alkaline solutions; and finally, deacetylation in concentrated alkaline solutions (Ahing and Wid, 2016b) (Ilyas and al ., 2022). Regardless of many years of commercialization, little is known about optimizing the isolation process, and there is no uniform method for isolating chitin and chitosan from shrimp waste. We require a commercially viable method that is efficient, rapid, and easily regulated to extract chitins of high purity and consistent quality for use in food and biomedical applications. There is still much work to get high-quality chitin, and chitosan back from waste goods used to make seafood. Response surface methodology (RSM) is a solid statistical tool for identifying variable interactions and optimizing chemical, biological, and other multifactorial processes (Younes and al ., 2014) (Nidheesh and Suresh, 2015). RSM was previously used to remove chitin from pink shrimp and crab shell powder. However, most research of (Nidheesh and Suresh, 2015) (Ben Seghir and Benhamza, 2017) (Al Shaqsi and al ., 2020), optimizes just deacetylation and demineralization steps. The three steps of optimizing the extraction of chitin and chitosan from crude shellfish byproducts using RSM have yet to be published, because (Aldila and al ., 2020) found that deacetylation is affected by deproteinization conditions. This study optimized the deceatylation and deacelyation conditions for chitosan extracted from shrimp waste for high quality/purity using RSM and a fractional factorial design. Time, temperature, and reagent concentration all influence the deacetylation of chitosan. However, this work aimed to explore the deproteinization and deacetylation in the manufacture of chitosan from shrimp waste using a fractional factorial design. The variables used in this design were temperature, concentration of NaOH, reaction time, particle size, and solid-liquid ratio. Everything revolved around making the levels better. No study uses a single factorial design to optimize these five chitin and chitosan extraction parameters in shrimp

shells. It should be noted that this work is a follow-up of our previous work: optimization of the demineralization of chitin (Kherbache and al ., 2022) .

2. Materials and methods

2.1. Materials

This study makes use of shrimp shells obtained from Tlemcen's fisheries and fishmonger. The shrimp shells were manually separated from the flesh, and washed in cold water to remove all impurities, before being sun-dried for two days. Using a blender, the dried shrimp shell samples were coarsely powdered at "0.3, 0.5 and 1 mm" in size. The coarse powder was keep in storage so that chitin could be made. The samples of coarse powder were demineralized (William and Wid, 2019).

2.2. Demineralization of chitin

This study is complementary to the preliminary study of the optimization of chitin demineralization of (Kherbache and al ., 2022), we optimized the demineralization conditions using a fractional factorial design 2^{5-1} (table 01), following the mandhods of, (Al Shaqsi and al ., 2020), with minor modifications. Each 40 g shrimp shells powdered sample (0.3 and 1 mm) were demineralized independently from sixteen Meyer Erlenes. All samples were treated with 1–2M HCl (1:10 and 1:15 w/v) at 25–50°C with continual stirring for 30–60 min. Demineralized samples were filtered, washed several times with distilled water, and oven-dried overnight at 50°C. After demineralization, materials were deproteinized.

Table 01: Factors and levels for the Fractional 2^{5-1} factorial design (Demineralization).

Factors	Code	Unit	Low level (-1)	High level (+1)
HCl Concentration	A	N	1	2
Temperature	B	°C	25	50
Reaction time	C	h	0.5	1
Particle size	D	mm	0.3	1
Solid/liquid ratio	E	g/ml	1/10	1/15

2.3. Deproteinization of chitin

Demineralized samples obtained were deproteinized using the established method (Aldila and al ., 2020), with slight modifications by treating them to different NaOH and Solid/liquid ratio concentrations, respectively (20 to 60%; 1:10 and 1:15 w/v). Under agitation for 30 and 60 min at 40 to 90°C temperature using a fractional factorial design 2^{5-1} (table 02). The sixteen samples were treated with deproteinization, followed by filtration and subsequent washing with distilled water. Subsequently, the deproteinized samples were dried in an oven for one night at a

temperature of 50°C. The samples that have undergone deproteinization were individually weighed with an analytical balance.

Table 02: Factors and levels for the Fractional 2^{5-1} factorial design (Deproteinization).

Factors	Code	Unit	Low level (-1)	High level (+1)
NaOH Concentration	A	%	20	60
Temperature	B	°C	40	90
Reaction time	C	min	30	60
Particles size	D	mm	0.3	1.0
Solid/Liquid ratio	E	g/ml	1/10	1/15

2.4. Deacetylation of chitin and obtention of chitosan

Deproteined samples obtained were deacandylated using the established method (Salman, Ulaiwi and Qais, 2018) With a few modifications. Chitin-isolated samples underwent treatment with sodium hydroxide (NaOH) solutions, ranging from 40-50% at 1:10-1:15(w/v) ratios. The treated samples were then placed in an autoclave and exposed to temperatures of 121°C and 130°C for 15 and 30 minutes, respectively. Using a fractional factorial design 2^{5-1} (table 03). After that, the samples were washed, filtered, and then dried in an oven for one night at a temperature of 50°C.

Table 03: Factors and levels for the Fractional 2^{5-1} factorial design (Deacetylation).

Factors	Code	Unit	Low level (-1)	High level (+1)
NaOH Concentration	A	%	40	50
Temperature	B	°C	121	130
Reaction time	C	min	15	30
Particles size	D	mm	0.3	1.0
Solid/Liquid ratio	E	g/ml	1/10	1/15

2.5. Characterization of prepared chitosan

2.5.1 Chitosan extraction yield

The estimation of chitosan yield was determined by dividing the dry weight of the produced chitosan by the wand weight of the initial shrimp shells, as expressed in equation (01) (Ahmed, Hassan and Nour, 2020).

$$\text{Yield } \% = \frac{\textbf{ExtractedChitosan (g)}}{\textbf{Shrimp Shell Waste } (g)} * \mathbf{100} \qquad (1)$$

2.5.2 Solubility in acid solution

The preparation of a homogeneous solution began with the dissolution of 1.0 g of chitosan, acquired by deacetylation, in 100 mL of 1% acetic acid (99%). The mixture was agitated using a magnetic stirrer until complete homogeneity was achieved. Subsequently, the solution of chitosan underwent filtration using a vacuum pump. The experiment was replicated on three separate occasions. The solubility % was determined using the following calculation (Ahing and Wid, 2016b):

$$\textit{Solubility } \% = \frac{(\textbf{ Initial weight of the tube + chitosan}) - (\textbf{Final weight of the tube +chitosan})}{(\textbf{Initial weight of the tube +chitosan}) - (\textbf{Initial weight of the tube})} * \mathbf{100} \qquad (02)$$

2.5.3 Residual Protein content determination

The nitrogen content was determined using the Kjeldahl technique. The determination of crude protein content included the multiplication of the nitrogen content, which was previously adjusted for any corrections by a factor of 6.25. The adjusted nitrogen content was obtained by subtracting the nitrogen content of chitin from the nitrogen in shrimp shell powder (Chang and Tsai, 1997).

2.5.4 Determination of chitosan deacetylation DD%

With a spectrum range of frequencies from 4000 to 400 cm-1, infrared spectroscopy (USA, Perkin Elmer Spectroscopy) is used to get the spectra of chitosan. After carefully combining the chitosan sample with KBr, the mixture is dried and pressed to create a homogenous sample/KBr disc. Equation 03 uses the absorption bands at 1655 and 3450 cm^{-1} to get the DD% (Ben Seghir and Benhamza, 2017):

$$\text{DD\% } = \mathbf{100} - \left[\mathbf{100} \times \frac{\left(\frac{\mathbf{A1655}}{\mathbf{A3450}}\right)}{\mathbf{1}} . \mathbf{33}\right] \qquad (03)$$

Where:

DD % is the degree of deacetylation, A1655 and A3450 cm^{-1} are the absolute heights of the amide and hydroxyl absorption bands. Fully acetylated chitosan has an A1655/A3450 ratio of 1.33.

2.5.5 Determination of intrinsic viscosity and molecular weight (Mw) of chitosan

The viscosity of the chitosan solution was measured using an osculated tube viscometer at a temperature of 25°C (Salman, Ulaiwi and Qais, 2018). The use of the provided equation determined the molecular weights (MW), and the outcomes are presented in centipoises (cPs) as indicated in equation (04).

$$\text{Mv } = \frac{\boldsymbol{\eta}}{\mathbf{k}} * \frac{\mathbf{1}}{\mathbf{a}} \qquad (04)$$

η: viscosity of the sample, 1.81×10-5 cm3/g and 0.93 the values of K and a respectively.

2.5.6 X-ray diffraction measurements

XRD was used to evaluate the crystallinity index and confirm the chitosan sample. An X-ray diffractometer (Rigaku X-ray diffraction equipment) analysis used 45 kV generating voltage and 40 mA tube current. Cu Kα radiation at λ = 1.5406Å was used to power the device, and samples were measured in the standard continuous mode at 2θ angles ranging from 05 to 45°. The step duration was 0.5 s, and the step size was 0.007°. Equation (07) was used to determine the crystallinity index (ICr) (Pădureţu and al ., 2019).

$$\mathbf{CIr} = \frac{\mathbf{I110-Iam}}{\mathbf{I110}} * \mathbf{100} \qquad (05)$$

Where: I110 represents the highest intensity at 2θ=20°, whereas Iam represents the amorphous diffraction intensity at 2θ=16°.

2.5.7 Scanning electron microscopy (SEM)

An SEM micrograph shows the morphology of the produced chitosan is carried out using a JEOL JCM-5000 scanning electron microscopy at 5 and 20 kV (Ben Seghir and Benhamza, 2017).

3. Statistical analysis

The response surfaces design approach (RSM) is used in this study's statistical analysis to establish an ideal DD% and lowest residual protein content to produce high-purity chitosan. Factor effects and second-order interactions are found using the fractional factorial design (FFD) applied using the selected (RSM) technique. The mathematical model is as follows (Younes and al ., 2014). The experimental design has sixteen factorial points, each with two levels defined –1 and +1 (Tables 02 and 03). The result that is derived is a second-order polynomial Eq. 08:

$$Y = a + \sum_{i=A}^{F} a_i x_i + \sum_{i=A\ j=A\neq i}^{F} a_{ij} x_i x_j + e \qquad (06)$$

Where: a0 is a constant, ai are the main effect coefficients for each factor, aij are the interaction effect coefficients, Y is the expected response, and xi are the encoded or coded values of the factors.

4. Results and discussion

4.1 Results

4.1.1. Optimization of extracting conditions by fractional factorial design (FFD)

4.1.1.1 Prediction model and statistical analysis

Table 04. Matrix of experiments, and results of deproteinization, deacetylation tests.

	Coded values					Responses		
Test	A	B	C	D	E	Residual proteins %	DD%	Yield %

1	-1	-1	-1	-1	1	12.38	81.37	11.68
2	1	-1	-1	-1	-1	13.61	81.61	13.36
3	-1	1	-1	-1	-1	11.92	83.08	14.61
4	1	1	-1	-1	1	13.19	81.3	15.93
5	-1	-1	1	-1	-1	3.00	82.52	15.61
6	1	-1	1	-1	1	3.59	80.75	15.72
7	-1	1	1	-1	1	7.45	80.81	15.53
8	1	1	1	-1	-1	5.41	80.86	15.67
9	-1	-1	-1	1	-1	5.41	80.63	15.73
10	1	-1	-1	1	1	2.60	80.46	13.96
11	-1	1	-1	1	1	11.47	80.48	14.90
12	1	1	-1	1	-1	5.31	80.51	13.09
13	-1	-1	1	1	1	3.30	80.49	15.79
14	1	-1	1	1	-1	12.04	80.6	13.65
15	-1	1	1	1	-1	6.50	80.84	15.57
16	1	1	1	1	1	3.11	80.53	13.42

The effect of the five variables on the residual proteins, the degree of deacetylation of chitosan (DD %), and the Yield of chitosan are examined simultaneously; the results are presented in Table 04. A response function model is created using the data from the fractional factorial design (FFD) and is stated as follows:

Residual protein% =+11.16+4.06* A+ 2.81* B-0.21* C + 2.09* D -1.17* E + 0.82* AB-0.43* AC + 0.20* BC + 0.51* BD - 0.79 * CD + 0.62* CE - 1.47* DE (07)

DD% =+81.05-0.23*A -1.250E - 003* B - 0.13* C - 0.49* D-0.28* E + 0.18* AD + 0.21* AE - 0.16* BC + 0.17* CD + 0.20* DE (08)

Yield % =+14.64 - 0.29A + 0.20B + 0.48C - 0.13D - 0.023E - 0.22AC - 0.70AD + 0.43AE - 0.27BC -0.47BD + 0.13BE - 0.39CD (09)

The encoded values of NaOH concentration, temperature, time of reaction, particle size, and solid/liquid ratio are denoted as A, B, C, D, and E, respectively.

Table 05. ANOVA for residual protein%.

Source	*Sum of Squares*	*df*	*Mean Square*	*F-Value*	*p-value Prob > F*	*conclusion*
Model	319.60	12	26.63	74.29	0.0023	significant
A-NaOHConentration	51.85	1	51.85	144.63	0.0012	significant
B-Temperature	26.30	1	26.30	73.37	0.0033	significant
C-Reaction time	**1.13**	**1**	**1.13**	**3.14**	**0.1745**	**Not significant**
D-Particle size	21.46	1	21.46	59.85	0.0045	significant
E-Solid/Liquid ratio	6.76	1	6.76	18.84	0.0226	significant
AB	6.85	1	6.85	19.12	0.0221	significant
AC	7.67	1	7.67	21.38	0.0190	significant
BC	**2.68**	**1**	**2.68**	**7.49**	**0.0716**	**Not significant**
BD	4.09	1	4.09	11.40	0.0432	significant
CD	39.69	1	39.69	110.72	0.0018	significant
CE	24.93	1	24.93	69.53	0.0036	significant
DE	34.68	1	34.68	96.74	0.0022	significant
Residual	3.76	4	0.94			
Cor Total	320.68	15				
Adj R-Squared	0.9830					
Pred R-Squared	0.9046					

Table 06. ANOVA for degree of deacetylation DD%.

Source	*Sum of Squares*	*df*	*Mean Square*	*F-Value*	*p-value Prob > F*	*conclusion*
Model	8.89	10	0.89	180.89	< 0.0001	significant
A-NaOH concentration	0.81	1	0.81	164.80	< 0.0001	significant
B-Temperature	2.500E-005	1	2.500E-005	5.086E-003	0.9459	Not significant
C-Time of reaction	0.26	1	0.26	52.92	0.0008	significant
D-Particle size	3.76	1	3.76	765.74	< 0.0001	significant
E-Solid/Liquid Ratio	1.24	1	1.24	252.95	< 0.0001	Significant
AD	0.53	1	0.53	108.42	0.0001	Significant
AE	0.71	1	0.71	145.27	< 0.0001	Significant
BC	0.43	1	0.43	87.29	0.0002	Significant
CD	0.49	1	0.49	99.69	0.0002	Significant
DE	0.65	1	0.65	131.85	< 0.0001	Significant
Residual	0.025	5	4.915E-003			
Cor Total	8.92	15				
Adj R-Squared	0.9917					
Pred R-Squared	0.9718					

Table 07. ANOVA for Yield%.

Source	*Sum of Squares*	*df*	*Mean Square*	*F-Value*	*p-value Prob > F*	*conclusion*
Model	*24.91*	*12*	*2.08*	*239.44*	*0.0004*	significant
A-NaOH concentration	*1.33*	*1*	*1.33*	*153.56*	*0.0011*	significant
B-Temperture	*0.66*	*1*	*0.66*	*75.88*	*0.0032*	significant
C-Time of reaction	*3.72*	*1*	*3.72*	*428.91*	*0.0002*	significant
D-particules size	*0.25*	*1*	*0.25*	*29.12*	*0.0125*	significant
E-Solid/Liquid ratio	***8.834E-003***	***1***	***8.834E-003***	***1.02***	***0.3871***	**Not significant**
AC	*0.75*	*1*	*0.75*	*86.77*	*0.0026*	significant
AD	*7.75*	*1*	*7.75*	*893.93*	*< 0.0001*	significant
AE	*2.99*	*1*	*2.99*	*344.50*	*0.0003*	significant
BC	*1.20*	*1*	*1.20*	*138.78*	*0.0013*	significant
BD	*3.55*	*1*	*3.55*	*409.42*	*0.0003*	significant
BE	*0.27*	*1*	*0.27*	*30.92*	*0.0115*	significant
CD	*2.43*	*1*	*2.43*	*280.45*	*0.0005*	significant
Residual	*0.026*	*3*	*8.669E-003*			
Cor Total	*24.93*	*15*				
Adj R-Squared	0.9948					
Pred R-Squared	0.9703					

FFD performed ANOVA analysis and F-test to evaluate the significance and fitness of the regression model Tables (05, 06 and 07). The results showed that the regression model for the three responses studied (residual proteins, DD%, and yield) was significant ($P < 0.05$). The R^2 value indicates that (99.62%, 99.72%, and 99.90%) the model explains the global variance. The "predicted R^2" value of (0.9042, 0.9917, and 0.9703) is probably the same as the "adjusted R^2" of

(0.9832, 0.9718, and 0.9948); the variance is less than 0.2. The model's F-value is calculated to be 74.29, 180.89, and 239.44. The argument suggests that the model has importance, and there is a limited probability (0.23%, 0.01%, and 0.04%) that such a high F-value could arise because of variation by chance.

4.1.1.2 Response surface plot

The influence of individual factors and the interaction of two variables on all three responses were investigated. Chitosan residual protein%, DD%, and yield% The data may be visually represented using of 3-dimensional (3D) response surface charts and two-dimensional (2D) contours plots. The provided graphs give a visual representation of regression models using graphical analysis.

•Response surface plot of residual protein%

The interactive effects observed are presented in Figure 01; the P values <0.05 for the four independent variables (A, B, D, and E) indicate a significant influence on the residual protein% and the interactions AB, AC, BD, CD, CE, DE exert a significant influence (P< 0.05). Nevertheless, the Temperature factor (C) and the interaction (BC) were not significant (P > 0.05). Interactions AB, AC, BD, CD, CE, and DE reveal that residual protein% decreases when NaOH concentration (A) temperature (B) particle size (D) decreases and time increases (C).

•Response surface plot of DD%

The interactive effects observed are presented in Fig.02; the P values <0.05 for the four independent variables (A, C, D, and E) indicate a significant influence on the DD%, the interactions AC, CD, CE, DE exert a significant influence (P>0.05). However, the variable (C) Temperature was not significant (P > 0.05). The interactions AD, AE, BC, CD, and DE reveal that DD% increases when the NaOH concentration (A), the reaction time (C), the particle size (D), and the Solid/Liquid ratio (E) decrease.

•Response surface plot of Yield %

Fig.03 shows that NaOH concentration (A), Temperature (B), reaction time (C), and particle size (D) have positive effects on the yield of chitosan. At the same time, the Solid/Liquid ratio (E) has a negative effect. For interactions: AC, BD, CD, CE, and DE have positive effects. Yield increases with decreasing factors A, B, C, and D. and increasing factors E.

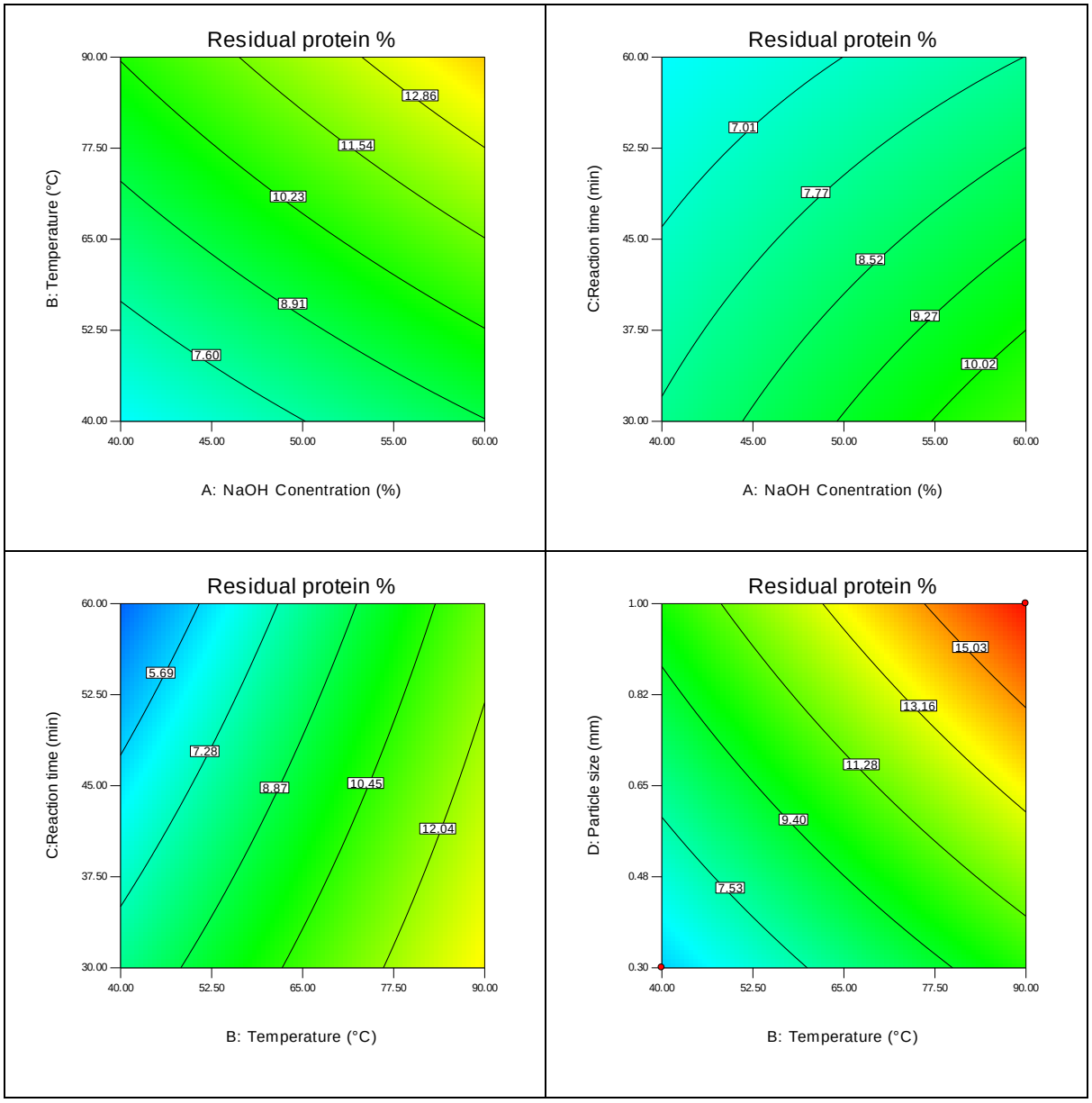
Residual protein %
B: Temperature (°C)
A: NaOH Conentration (%)
12,86
11,54
10,23
8,91
7,60
90.00
77.50
65.00
52.50
40.00
40.00
45.00
50.00
55.00
60.00
Residual protein %
C:Reaction time (min)
A: NaOH Conentration (%)
7,01
7,77
8,52
9,27
10,02
60.00
52.50
45.00
37.50
30.00
40.00
45.00
50.00
55.00
60.00
Residual protein %
C:Reaction time (min)
B: Temperature (°C)
5,69
7,28
8,87
10,45
12,04
60.00
52.50
45.00
37.50
30.00
40.00
52.50
65.00
77.50
90.00
Residual protein %
D: Particle size (mm)
B: Temperature (°C)
15,03
13,16
11,28
9,40
7,53
1.00
0.82
0.65
0.48
0.30
40.00
52.50
65.00
77.50
90.00

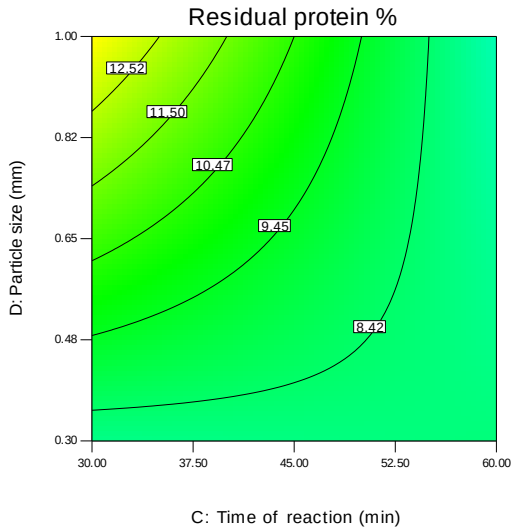

Fig. 01: Contour graphs for variable effects on Residual protein %

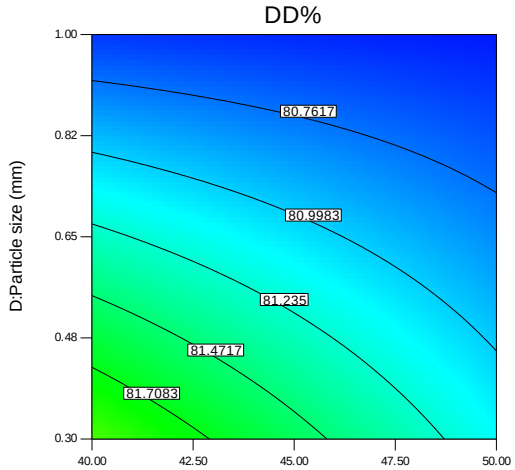

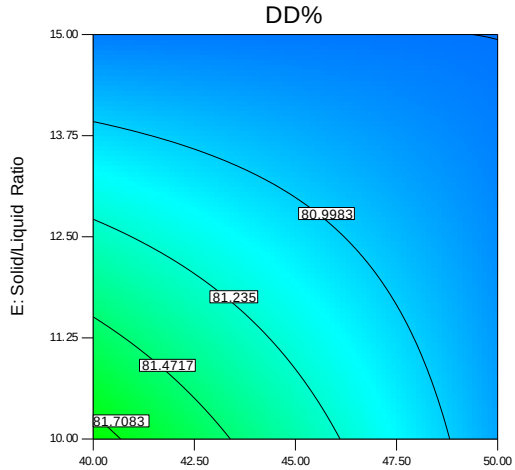

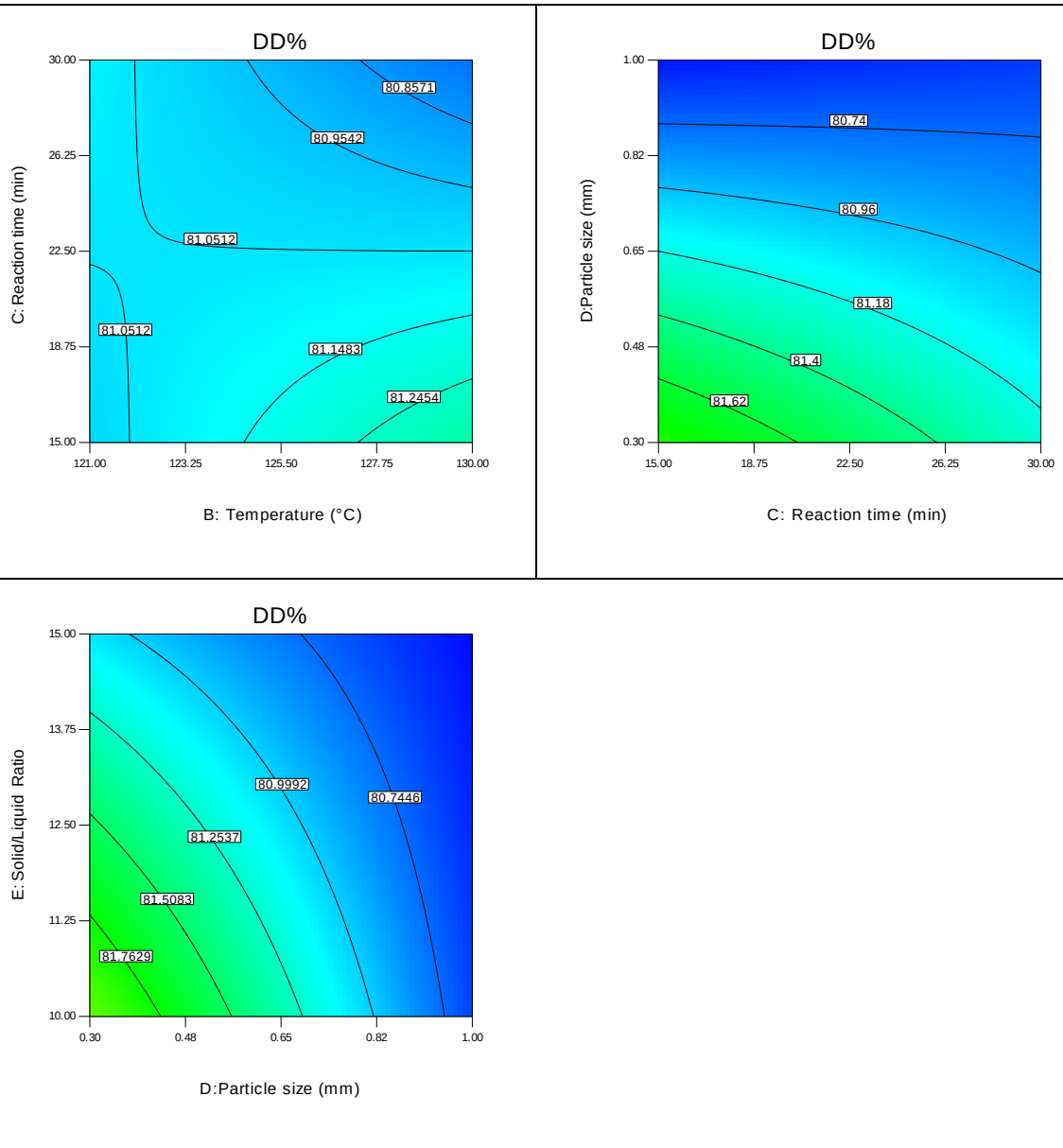

Fig. 02: Contour graphs for variable effects variables on DD%

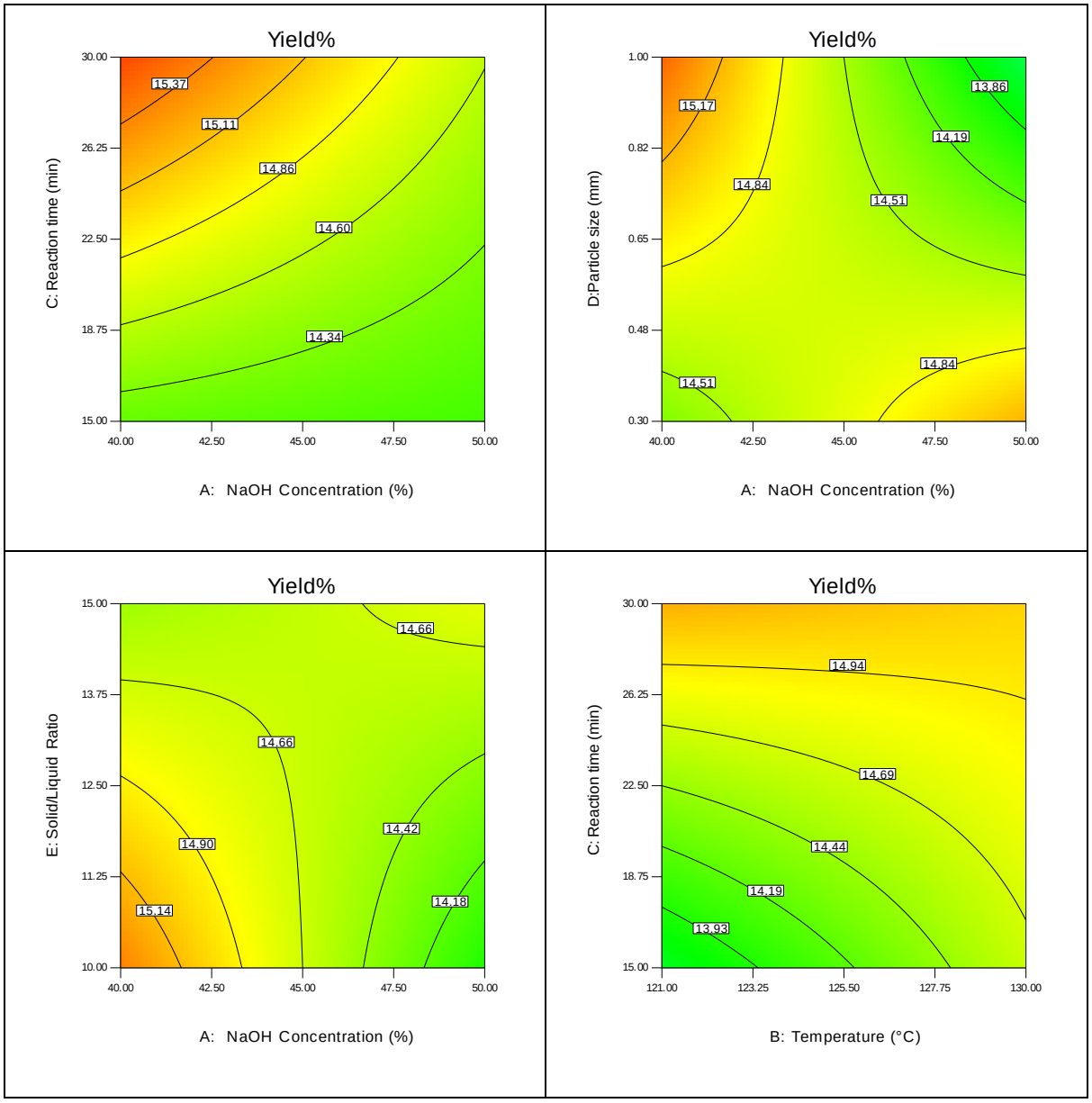
Yield%
C: Reaction time (min)
A: NaOH Concentration (%)
15.37
15.11
14.86
14.60
14.34
Yield%
D:Particle size (mm)
A: NaOH Concentration (%)
15.17
14.84
14.51
14.19
13.86
14.84
14.51
Yield%
E: Solid/Liquid Ratio
A: NaOH Concentration (%)
14.66
14.66
14.90
14.42
15.14
14.18
Yield%
C: Reaction time (min)
B: Temperature (°C)
14.94
14.69
14.44
14.19
13.93

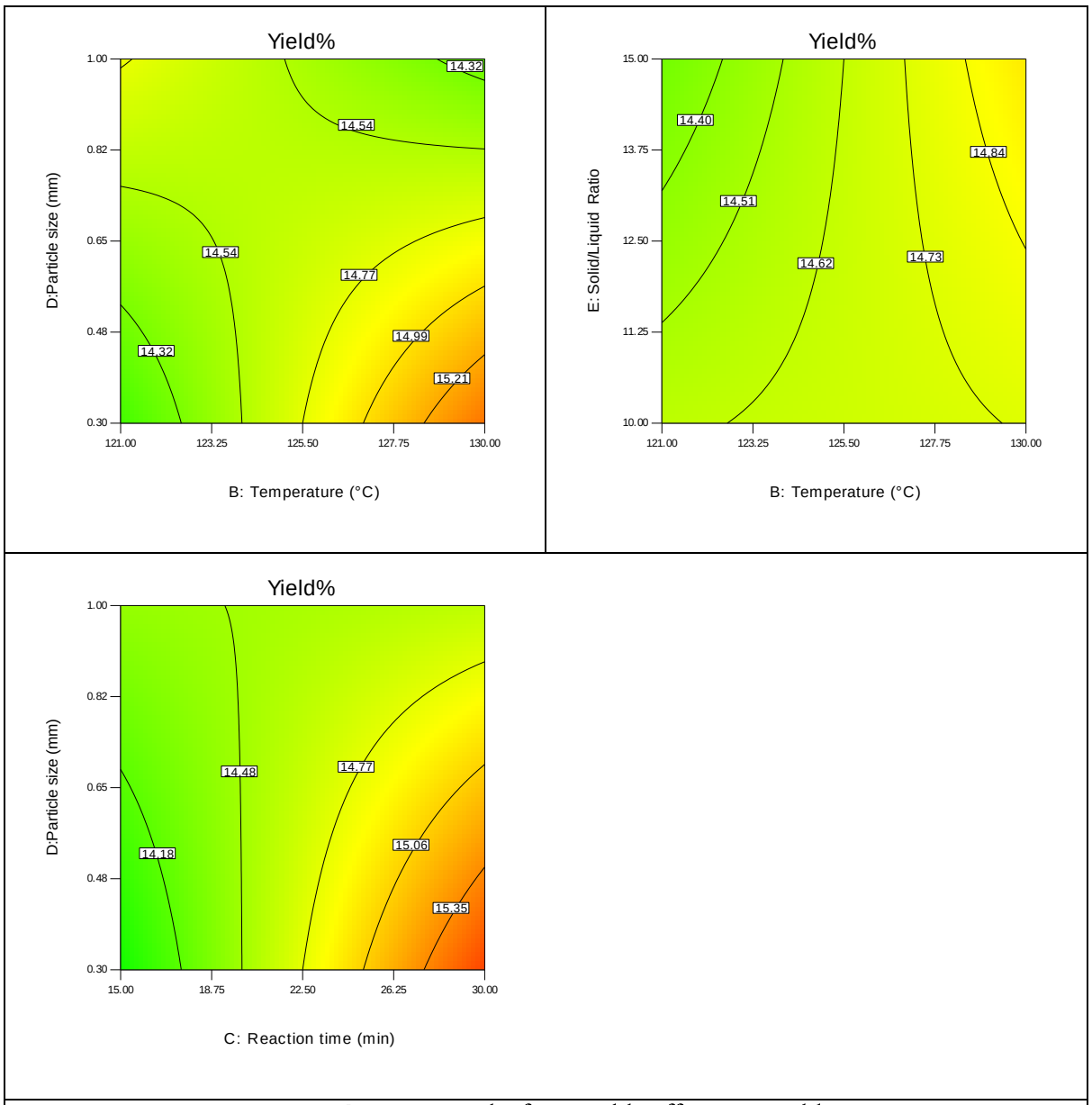

Fig. 03: Contour graphs for variable effects on Yield %

4.1.1.3 Optimization using the desirability function

In order to improve and validate the precision of the predicted mathematical model, expertly designed experiments were carried out under identical experimental settings. As the desirability function is increased, the model's accuracy improves, and the optimal parameters with a desirability value of 1.000 and 0.904 correspond to a residual protein % of 2.45%, a DD% of 83.09% and a yield of 14.52 (Fig.04, 05 and 06). The optimal chitin demineralization condition for chitosan extraction was 2N HCl concentration, 50°C for temperature, reaction time 0.5 h, 1 mm particle size, Solid/Liquid ratio of 1/10 g/l , actual values of yield, and ash content was 39.77%, 0.14% respectively (Kherbache and al ., 2022). The minimum residual proteins reached under these conditions correspond to the concentration of NaOH 20%, temperature of 40°C, reaction time

of 60 minutes, particle size of 1.00 mm, and Solid/Liquid ratio of 1/15 g/ml. The maximum degree of deacetylation DD% and the yield% reached at a NaOH concentration of 40%, temperature of 129.88°C, a reaction time of 15.03 minutes, particle size of 0.3 mm, and Solid/Liquid ratio of 1/10.02 g/ml. Under these conditions, chitosan samples are prepared, and characterization techniques are carried out.

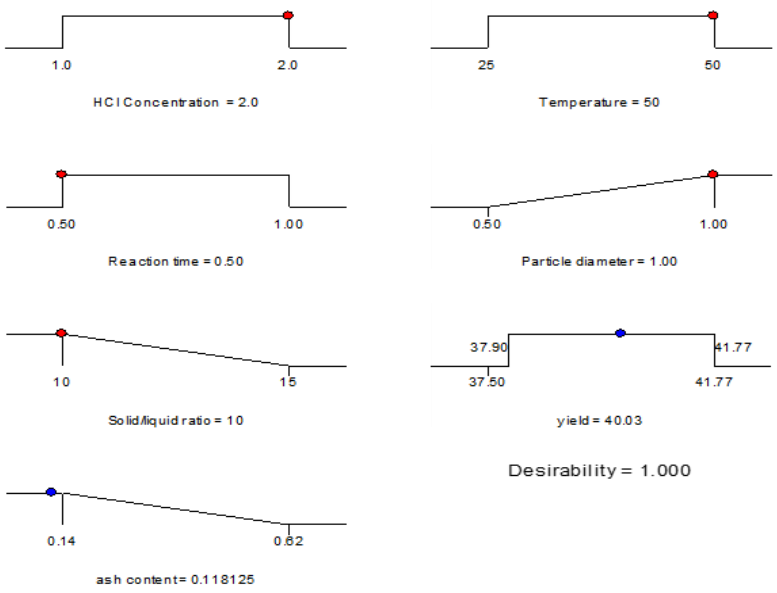

Fig.04: Desirability ramp for optimization of demineralization.

HCl (N), temperature (°C), reaction time (min), particles size (mm), and Solid/Liquid ratio (g/ml)

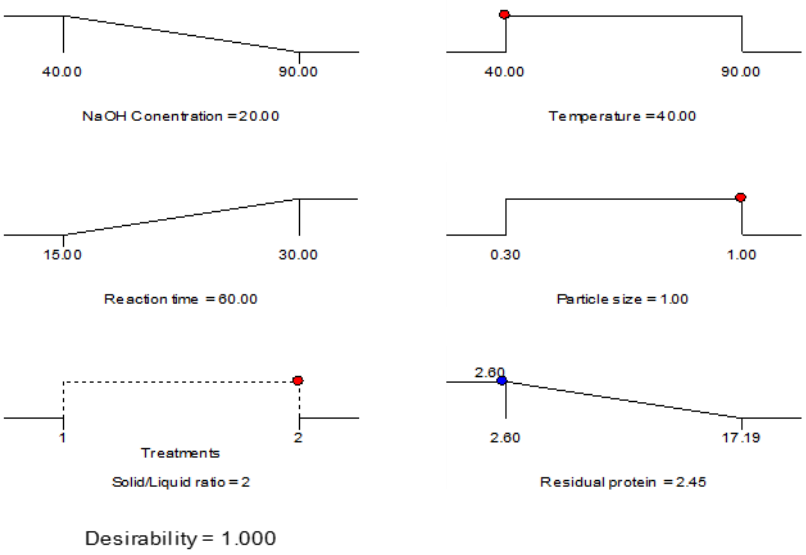

Fig.05: Desirability ramp for optimization of deproteinization

NaOH (%), temperature (°C), reaction time (min), particles size (mm), and Solid/Liquid ratio (g/ml)

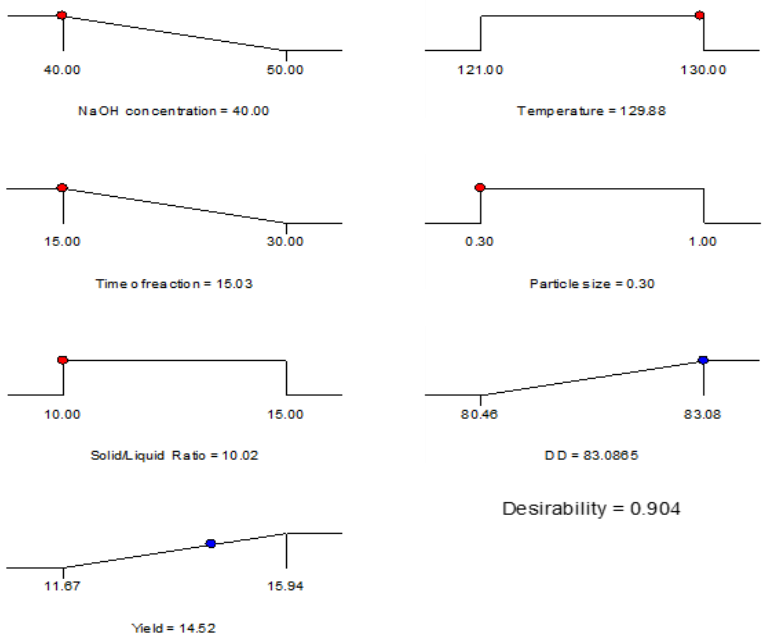

Fig.06: Desirability ramp for optimization of deacetylation

NaOH (%), temperature (°C), reaction time (min), particles size (mm), and Solid/Liquid ratio (g/ml)

4.1.1.4 Chitosan characterization

Chitosan samples that are produced under optimal conditions are analyzed using biochemical quality analysis, Scanning electron microscopy (SEM), X-ray diffraction (DRX), and Fourier-transform infrared spectroscopy (FTIR) methods for characterization.

•Moisture, protein, ash and Molecular weight of chitosan

The biochemical quality analysis evaluated the efficiency of several optimized conditions in producing chitosan from shrimp shell waste. These conditions included demineralization, deproteinization, and deacetylation. Table 08 presents the quantitative data about the moisture, protein, ash content, molecular weight, solubility, and degree of deacetylation of chitosan. The chitosan yield obtained in this study was 16.16±0.22%, which is comparatively lower than the yield reported by (Al-Hasan Hamdan and al ., 2020). The discovery yielded a proportion of 18-19%. The observed decrease in size may be attributed to the chitosan polymer's depolymerization, the reduction in mass resulting from excessive acetyl group removal during deacetylation, and the loss of chitosan particles during the washing process. The chitosan had a moisture content of 5.77±0.08%. This finding shows the ability of chitosan to adsorb moisture from the environment around it successfully. Chitosan shows hygroscopic characteristics due to its ability to form hydrogen bonds with water molecules, facilitated by certain chemical groups within its structure

(Salman, Ulaiwi and Qais, 2018). An increased conservation time for chitosan was attained by keeping a moisture content value below 10% (Nouri and al ., 2016). The present study produced a chitosan sample with an ash content of 0.124±0.002%. High-quality chitosan's highest acceptable ash proportion was below 1% (Ghannam and al ., 2016). Moreover, there is an unambiguous relationship between chitosan ash content and the demineralization process's efficacy. The chitosan had a protein content of 2.08±0.05%. The previous statement relates to evaluating deproteinization efficiency in synthesizing chitosan. The average molecular weight of chitosan, determined by related viscosity, was found to be 107.47±0.44 (KDa). In general, the molecular weight of chitosan exceeds one million, although commonly accessible chitosan compounds show a range of 100 KDa to 1200 KDa (Renuka and al ., 2019). Because chitosan is a combination of two polymers (chitin and chitosan) that have various solubility features, the solubility, which is 97.02±0.09%, is directly dependent on the degree of deacetylation and the molar mass. It is proposed that as the degree of deacetylation increases, the chitosan concentration increases and produces more amino groups, which increase the solubility in acetic acid solutions (Pădureţu and al ., 2019).

Table 08: Physiochemical Properties of chitosan

Yield %	Moisture %	Ash %	Protein%	M.W Kda	Solubility %	DD %
16.16±0.22	5.77±0.08	0.124±0.002	2.08±0.05	107.47±0.44	97.02±0.09	87.13±0.16

•FTIR spectroscopy

FTIR analysis confirmed the synthesized chitosan's structure. As shown in Fig.07, the spectra of chitosan show a large absorption band in the 3443.16 cm^{-1} area, which is suggestive of the NH stretching vibrations of free amino groups and the OH stretch vibrations of water and hydroxyls. The spectral peak seen at a wavenumber of 2924.14 cm^{-1} may be attributed to the asymmetric stretching vibrations of the CH_3 and CH_2 functional groups in the synthesized chitosan sample (Mohanasrinivasan and al ., 2014). The significant peak observed at a wavenumber of 1652.32 cm^{-1} may be attributed to the stretching vibration of the NH_2 group. This vibrational mode is restricted to chitosan polysaccharides and is a marker of the deacetylation process (Ahing and Wid, 2016a). C–H stretching is shown by the peak at 1421.39 cm^{-1}, while an amide III coming from N-acetyl-glucosamine's C–N stretching is seen at 1380.90 cm^{-1}. The absorption peak at 1152.25 cm^{-1} shows a symmandrical glycosidic bond (C–O–C), and a further absorption band is shown at 1027 cm^{-1}, which shows a stretching vibration of the C ring. The glycosidic bond of the β-anomer (1–4) (C–O–C) is identified by the absorption peak at about 896.13 cm^{-1} (Ben Seghir and Benhamza, 2017).

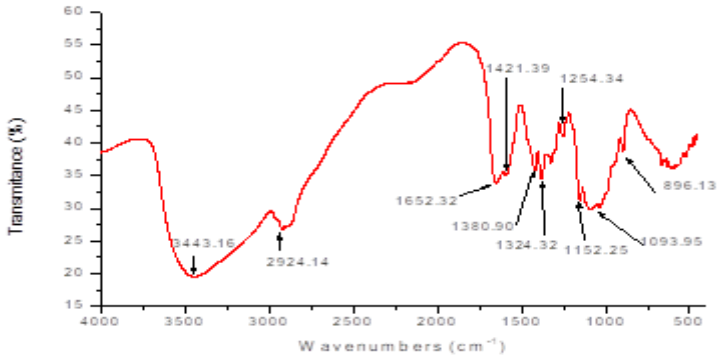

Fig.07: FTIR of prepared chitosan by optimized conditions.

•X-ray diffraction analysis

X-ray diffraction (XRD) analysis was used to determine the degree of crystallinity shown by chitosan samples produced under optimized conditions. Fig.08 illustrates the selected chitosan sample's X-ray diffraction (XRD) pattern. The X-ray diffraction (XRD) analysis of chitosan showed the presence of two distinct crystal peaks at 9.9° and 20°. These peaks closely resemble the results reported by (Dahmane and al ., 2014). The degree of crystallinity observed in the produced chitosan was found to be 44.32%. The observed drop in value may be related to the presence of hydrogen intermolecular bonds after the deacetylation step. This occurrence suggests that the product's molecular structure is in an amorphous form (Ben Seghir and Benhamza, 2017). The results show that excessive deacetylation temperatures exert a negative impact on the hydrogen bonds present in the chitin structure, leading to a decrease in crystallinity (Ibitoye and al ., 2018).

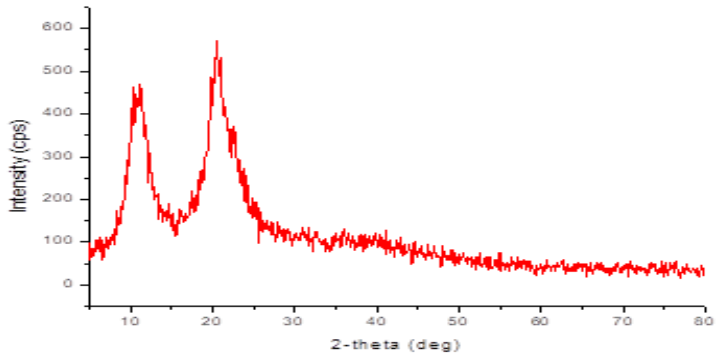

Fig.08: X-ray diffraction patterns of chitosan prepared by optimized conditions.

•Scanning electron microscopy (SEM)

SEM examined the structure of chitosan at various magnifications; Figure 09 illustrates the various areas. According to these findings, the chitosan's surface shape was rigorous and had fibrous veins, consistent with the findings (Chen and al ., 2021). Additionally, they have a porous structure that

has the potential to facilitate many applications, such as the adsorption of dyes and metal ions (Hong and al ., 2018).

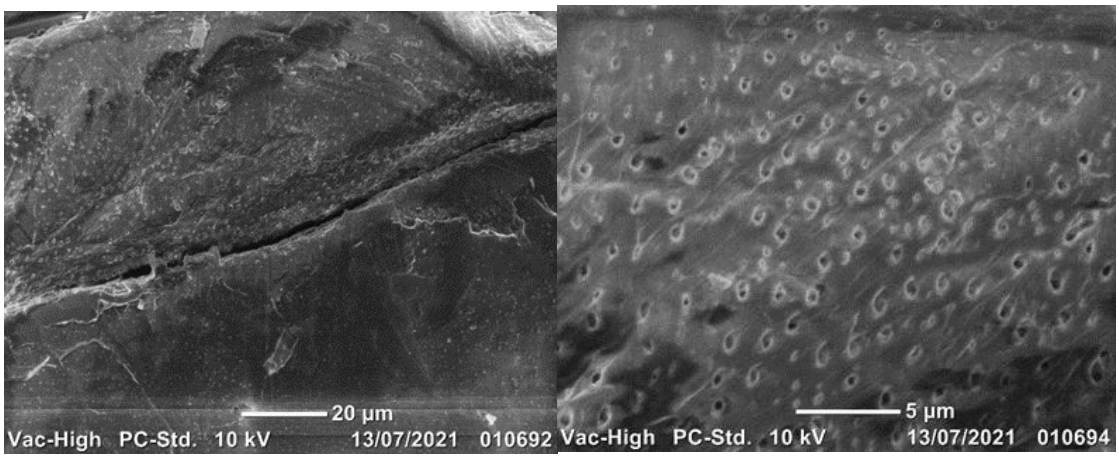

Fig.09: The SEM of chitosan at 20 and 05µm.

4.2. Results and comparison

The optimization of deproteinization and deacetylation of chitin was affected by the parameters of five process variables, such as NaOH concentration, temperature, reaction time, particle size, and solid/liquid ratio, as shown by the findings of this research. The residual of ash and proteins are 0.124±0.002% and 2.08±0.05%., respectively, and the DD% obtained is 87.13±0.16%. These results present an excellent discovery compared to those of previous studies. The ash content obtained 0.124±0.002% is comparatively lower than that found by (Salman, Ulaiwi and Qais, 2018),(Trung and al ., 2020), Which were 1.2, 0.72, and 0.3%, respectively. The low protein values indicate the effectiveness of the deproteinization step followed in preparing chitin for protein removal (No, Meyers and Lee, 1989). The protein content of the raw material is about 37.33±0.5% after treatment with NaOH reduced to values ranging to 2.08±0.05%. This result is lower than the 5% and 2.3% reported for Shells of pink shrimps (Solenoceramelantho) and Newfoundland pink shrimp (Shahidi and Synowiecki, 1991),(Chang and Tsai, 1997). The optimized DD% (87.13±0.16%) values are comparatively higher than those found in the studies of (Pădureţu and al ., 2019),(Poothawan and Lomthaisong, 2015), with obtained DD% of 82.5 86.13%, respectively. Comparisons conducted with other research studies reveal that an essential number of investigations often use a restricted sand of three to four variables (Al Shaqsi and al ., 2020),(Pădureţu and al ., 2019),(Ben Seghir and Benhamza, 2017), less than that of our work where we optimize the three stages of the extraction, we use the five mainly significant variables.

5. Conclusions

The experimental methodology aims to minimize the residual proteins, maximize the Deacetylation DD%, and yield in chitosan extraction. The effect of the five factors (NaOH

concentration, temperature, reaction time, particle size and, Solid/Liquid ratio) generated a first-order equation, the estimated yield and residual protein%, the DD%, and the yield% presented a good fit, with high correlations (R>98%). The results show that the minimum residual proteins reached under these conditions correspond to the concentration of NaOH 20%, the temperature of 40°C, reaction time of 60 minutes, particle size of 1.00 mm, and Solid/Liquid ratio of 1/15 g/ml. The maximum degree of deacetylation DD% and the yield% reached at a NaOH concentration of 40%, temperature of 129.88°C, a reaction time of 15.03 minutes, particle size of 0.3 mm, and Solid/Liquid ratio of 1/10.02 g/ml. After carrying out the validation test, the chitosan obtained presents a yield, ash rate, residual proteins, a DD%, solubility, crystallinity, and a molecular weight of 16.16±0.22, 0.124±0.002, 2.08±0.05%, 87.13±0.16%, 97.02±0.09%, 44.32%, and 107.47±0.44KDa respectively. This study proved that this methodology was adequate to obtain high-quality (>98%) chitin and chitosan from shrimp processing raw wastes and reduce industrial extraction time.

Acknowledgment

The authors would like to acknowledge, the Algerian Ministry of Higher Education and Scientific Research (MERSRS) and the General Directorate of Scientific Research and Technological for the financial and technical support.

Author contributions

Atiqa Kherbache and Linda Ouided Ouahab: performed the experiments, created the statistical analysis, mathematical models and prepared the paper. Fatma Youcefi: supervised the experiments, Project administration, Supervision, critically read the manuscript. Ouided Dehhas and Achref Cherifi: helped in the characterization of chitins and chitosan. All authors have read and approved the manuscript.

Data availability

This published article contains all of the data generated or analyzed during this study.

Declarations

Funding: The authors declare that they have no funding received.

Conflict of interest: The authors declare that they have no conflict of interest.

References:

[1] Ahing FA, and Wid N (2016a) 'Extraction and Characterization of Chitosan from Shrimp Shell Waste in Sabah', 3(Figure 1), pp. 227–237.
[2] Ahing FA and Wid N (2016b) 'Optimization of shrimp shell waste deacetylation for chitosan production', International Journal of ADVANCED AND APPLIED SCIENCES, 3(10), pp. 31–36. doi: 10.21833/ijaas.2016.10.006.
[3] Ahmed A, Hassan A, and Nour M (2020) 'Utilization of chitosan extracted from shrimp shell waste in wastewater treatment as low cost biosorbent', Egyptian Journal of Chemistry, 0(0), pp. 0–0. doi: 10.21608/ejchem.2020.43166.2871.

[4] Al-Hasan Hamdan and al (2020) 'Extraction, characterization and bioactivity of chitosan from farms shrimps of Basra province by chemical mandhod', Journal of Physics: Conference Series, 1660(1). doi: 10.1088/1742-6596/1660/1/012023.
[5] Aldila H and al (2020) 'The effect of deproteinization temperature and NaOH concentration on deacetylation step in optimizing extraction of chitosan from shrimp shells waste', IOP Conference Series: Earth and Environmental Science, 599(1). doi: 10.1088/1755-1315/599/1/012003.
[6] Chang KLB, and Tsai G (1997) 'Response Surface Optimization and Kinandics of Isolating Chitin from Pink Shrimp (Solenoceramelantho) Shell Waste', Journal of Agricultural and Food Chemistry, 45(5), pp. 1900–1904. doi: 10.1021/jf9606870.
[7] Chen S and al (2021) 'Preparation of antioxidant and antibacterial chitosan film from periplananda Americana', Insects, 12(1), pp. 1–14. doi: 10.3390/insects12010053.
[8] Dahmane EM, and al (2014) 'International Journal of Polymer Analysis and Characterization Extraction and Characterization of Chitin and Chitosan from Parapenaeuslongirostris from Moroccan Local Sources', (December), pp. 37–41. doi: 10.1080/1023666X.2014.902577.
[9] FAO (2019) FAO Yearbook. Fishery and Aquaculture Statistics 2019/FAO annuaire. Statistiques des pêches and de l'aquaculture 2019/FAO anuario. Estadísticas de pesca y acuicultura 2019. doi: 10.4060/cb7874t.
[10] Ghannam HE, and al (2016) 'Characterization of Chitosan Extracted from Different Crustacean Shell Wastes', Journal of Applied Sciences, 16(10), pp. 454–461. doi: 10.3923/jas.2016.454.461.
[11] Hong S, and al (2018) 'Versatile acid base sustainable solvent for fast extraction of various molecular weight chitin from lobster shell', Carbohydrate Polymers, 201, pp. 211–217. doi: 10.1016/j.carbpol.2018.08.059.
[12] Ibitoye EB, and al (2018) 'Extraction and physicochemical characterization of chitin and chitosan isolated from house crickand', Biomedical Materials (Bristol), 13(2). doi: 10.1088/1748-605X/aa9dde.
[13] Ilyas RA, and al (2022) 'Nanocomposites for Various Advanced Applications'.
[14] Kannan S, Gariepy Y, and Raghavan GSV (2017) 'Optimization and Characterization of Hydrochar Derived from Shrimp Waste', Energy and Fuels, 31(4), pp. 4068–4077. doi: 10.1021/acs.energyfuels.7b00093.
[15] Kherbache A, and al (2022) 'Optimization of chitin demineralization from shrimp shells waste by Response Surface Mandhodology (RSM)', South Asian Journal of Experimental Biology, 12(5), pp. 725–734. doi: 10.38150/sajeb.12(5).p725-734.
[16] Mohanasrinivasan V, and al (2014) 'Studies on heavy mandal removal efficiency and antibacterial activity of chitosan prepared from shrimp shell waste', 3 Biotech, 4(2), pp. 167–175. doi: 10.1007/s13205-013-0140-6.
[17] Nidheesh T, and Suresh PV (2015) 'Optimization of conditions for isolation of high quality chitin from shrimp processing raw byproducts using response surface mandhodology and its characterization', Journal of Food Science and Technology, 52(6), pp. 3812–3823. doi: 10.1007/s13197-014-1446-z.

[18] No HK, Meyers SP, and Lee KS (1989) 'Isolation and Characterization of Chitin from Crawfish Shell Waste', Journal of Agricultural and Food Chemistry, 37(3), pp. 575–579. doi: 10.1021/jf00087a001.
[19] Nouri M and al (2016) 'Improvement of chitosan production from Persian Gulf shrimp waste by response surface mandhodology', Food Hydrocolloids, 59, pp. 50–58. doi: 10.1016/j.foodhyd.2015.08.027.
[20] Pădureţu C, cezarina and al (2019) 'Influence of the paramanders of chitin deacetylation process on the chitosan obtained from crab shell waste', Korean Journal of Chemical Engineering, 36(11), pp. 1890–1899. doi: 10.1007/s11814-019-0379-7.
[21] Poothawan T, and Lomthaisong K, (2015) 'Analysis of chitin, chitosan, and optimization for carotenoids extraction yield with rice bran oil from thai fairy shrimp', Chiang Mai Journal of Science, 42(4), pp. 918–929.
[22] Renuka V, and al (2019) 'Production and Characterization of Chitosan from Shrimp Shell Waste of Parapeneopsisstylifera', International Journal of Current Microbiology and Applied Sciences, 8(11), pp. 2076–2083. doi: 10.20546/ijcmas.2019.811.240.
[23] Salman DD, Ulaiwi WS, and Qais A (2018) 'Preparation of chitosan from Iraqi shrimp shell by autoclave, studying some physiochemical properties and antioxidant activity', Journal of Pharmaceutical Sciences and Research, 10(12), pp. 3120–3123.
[24] Ben Seghir B and Benhamza MH (2017) 'Preparation, optimization and characterization of chitosan polymer from shrimp shells', Journal of Food Measurement and Characterization, 11(3), pp. 1137–1147. doi: 10.1007/s11694-017-9490-9.
[25] Shahid F, and Synowiecki J (1991) 'Isolation and Characterization of Nutrients and Value-Added Products from Snow Crab (Chinoecandes Opilio) and Shrimp (Pandalus Borealis) Processing Discards', Journal of Agricultural and Food Chemistry, 39(8), pp. 1527–1532. doi: 10.1021/jf00008a032.
[26] Al Shaqsi NHK, and al. (2020) 'Optimization of the demineralization process for the extraction of chitin from Omani Portunidae segnis', Biochemistry and Biophysics Reports, 23(July), p. 100779. doi: 10.1016/j.bbrep.2020.100779.
[27] Trung TS, and al (2020) 'Improved mandhod for production of chitin and chitosan from shrimp shells', Carbohydrate Research, 489(January), p. 107913. doi: 10.1016/j.carres.2020.107913.
[28] William W, and Wid N (2019) 'Comparison of extraction sequence on yield and physico-chemical characteristic of chitosan from shrimp shell waste', Journal of Physics: Conference Series, 1358(1). doi: 10.1088/1742-6596/1358/1/012002.
[29] Younes I and al (2014) 'Use of a fractional factorial design to study the effects of experimental factors on the chitin deacetylation', International Journal of Biological Macromolecules, 70, pp. 385–390. doi: 10.1016/j.ijbiomac.2014.06.051.